Since January 2020 Elsevier has created a COVID-19 resource centre with free information in English and Mandarin on the novel coronavirus COVID-19. The COVID-19 resource centre is hosted on Elsevier Connect, the company's public news and information website.

Available online at www.sciencedirect.com
ScienceDirect
Biochimica et Biophysica Acta 1774 (2007) 781–791
Biochimica et Biophysica Acta
BBA
www.elsevier.com/locate/bbapap

Helicity propensity and interaction of synthetic peptides from heptad-repeat domains of herpes simplex virus 1 glycoprotein H: A circular dichroism study

Barbara Sanavio [a], Angela Piccoli [a], Tatiana Gianni [b], Carlo Bertucci [a,*]

[a] Department of Pharmaceutical Chemistry, University of Bologna, via Belmeloro 6, 40126, Bologna, Italy
[b] Department of Experimental Pathology, Section of Microbiology and Virology, via San Giacomo 12, 40126, Bologna, Italy

Received 8 September 2006; received in revised form 20 March 2007; accepted 17 April 2007
Available online 22 May 2007

Abstract

The secondary structure of two synthetic peptides from heptad-repeat domains of herpes simplex virus 1 glycoprotein H was determined by circular dichroism. In particular, the propensity of these peptides to assume an ordered structure was investigated upon by changing the solvent's polarity and the temperature. A reduction of solvent polarity led to a significant increase in the α-helix content in the case of HR1, whereas only a slight change in the secondary structure was observed in the case of HR2. In both cases the conformational change followed a two-state transition model. The interaction of the peptides was monitored by the conformational change in the mixture with respect to the single peptides. However, formation of the complex did not significantly enhance thermal stability. A reliable estimation of the secondary structure was obtained by optimising the experimental conditions to collect CD data down to 180 nm, and by comparing the structure data yielded by different software packages.

Keywords: Circular dichroism; Secondary structure estimation; Peptide-peptide complexes; Thermal denaturation; Peptide folding

1. Introduction

Enveloped virus infection resides in fusion of the viral and eukaryotic membranes. This is triggered by viral fusion glycoproteins that help to overcome the highly energetic barrier due to the inherent stability of the lipid bilayer [1]. How fusion proteins act is an ongoing topic of research and discussion.

The fusion protein of influenza virus, hemagglutinin, has emerged as a sort of paradigm of Class I proteins. Even though the fusion proteins belonging to this class, like hemagglutinin, HIV gp41, SARS-CoV glycoproteins, and paramyxovirus F protein [1] are not well correlated in terms of sequence homology [2], they share some common structural and functional features. In particular, Class I fusion glycoproteins contain two key structural elements. The hydrophobic fusion peptide domain can penetrate the target membrane thereby forming a bridge between the two membranes [1–3]. Downstream of the target membrane, two other sequences called Heptad Repeats (HR) are involved in the steps leading to lipid mixing and membrane fusion [1–3]. The two HRs consist of seven-amino acids arrays where the first and fourth positions are occupied by hydrophobic residues determining a strong propensity to assume a α-helical conformation as solvent polarity decreases and the hydrophobic positions become exposed. These stretches, generally named N-terminal (HR1) and C-terminal (HR2), are usually located downstream of the fusion peptide and upstream from the transmembrane domain respectively. As the protein is assumed to trimerize to trigger fusion [1,2], the crucial refolding leads to the formation of a triple helical coiled-coil structure (a six-helix bundle) due to the interaction of three C-term HRs with a trimeric core of N-term HRs.

Herpes Simplex Virus type I (HSV) entry into the eukaryotic cell requires a pool of glycoproteins not yet completely characterized, four of which are essential for the fusion mechanism [3,4]. After target recognition upon the interaction of gD and one of the cell receptors, a complex concerted mechanism involves three other glycoproteins, namely gB, gH and gL. The emerging

* Corresponding author. Tel.: +39 051 2099742; fax:+39 051 2099734.
E-mail address: carlo.bertucci@unibo.it (C. Bertucci).

1570-9639/$ - see front matter © 2007 Elsevier B.V. All rights reserved.
doi:10.1016/j.bbapap.2007.04.019

role of gH as the executor of fusion triggers a deeper characterization of the key structural elements of this viral fusion protein. Recent works have identified gH's fusion peptide and HRs. In particular, the HRs of gH were characterized first by bioinformatic prediction and then by in vitro studies of mutagenesis and inhibition/reversion of infectivity. The bioinformatic search posed the N-terminal HR with a high propensity to assume a coiled-coil conformation, called HR-1, at residues 443–475, while HR-2 was located at amino acids 556–585. Site-specific mutagenesis and sequence substitution revealed the crucial role in viral fusion. To elucidate the details of the whole mechanism, synthetic peptides mimicking the native sequences involved in fusion are widely used also because of the major therapeutic implications arising from the development of peptidomimetic drugs. Many systems have been investigated through this path ([1,2], and, as an example, ref. [5]). Two synthetic peptides of 25 aa each, gH-HR1–25 (444–468, abbr. HR1–25) and gH-HR2–25 (556–580, abbr. HR2–25), have already been tested in vitro for their ability to reduce viral infection, and in particular viral fusion, and to prove their reciprocal interaction, as demonstrated by NPAGE and reversion of infectivity inhibition [6].

This study used circular dichroism (CD) spectroscopy to confirm and investigate the helicity propensity of the two peptides in depth. The interaction between the two peptides was monitored under different experimental conditions, in terms of polarity of the solvent and temperature. A reliable estimation of the secondary structure was obtained by optimising the experimental conditions to collect CD data down to 180 nm, and by comparing the structure data yielded by different software packages.

2. Materials and methods

2.1. Chemicals

Phosphate buffered saline (PBS), final pH 7.4, was prepared using Sigma dry powder in tablets. Each tablet dissolved in 200 ml of deionised water yields 0.01 M phosphate buffered saline, NaCl 0.137 M, KCl 0.0027 M, pH 7.4 at 25 °C. Na_2HPO_4, NaH_2PO_4, Na_2SO_4, KCl, NaCl powder were purchased from Carlo Erba Reagenti (Milan, Italy), while 2,2,2 trifluoroethanol (TFE) and acetonitrile (ACN) were from Fluka (Sigma-Aldrich, Milan, Italy). All solutions were prepared using bidistilled water and buffers were also filtered in a vacuum pump system using 0.2 μm pore membrane filters (Millipore, Milan, Italy). Helmanex II was supplied by Hellma (Milan, Italy). All other reagents were of analytical grade.

2.2. CD measurements

CD measurements were performed on a Jasco J-810 spectropolarimeter (Jasco, Japan) using Suprasil quartz cells. After each analysis the cells were repeatedly rinsed with water and ethanol, and after each set were filled with a 1% solution of Helmanex II for at least 1 h at room temperature to remove any

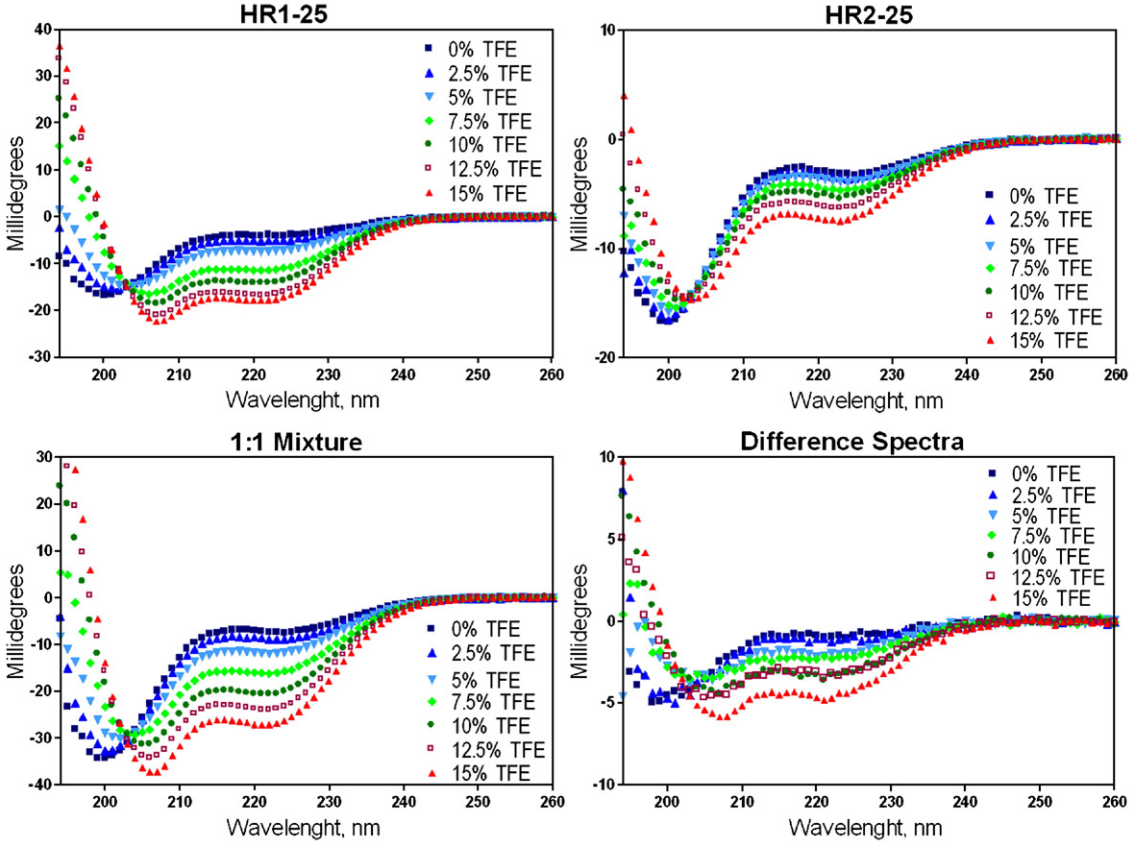

Fig. 1. CD spectra of HR1–25 (A), of HR2–25 (B), and of their 1/1 mixture (C): [peptide] 50 μM, PBS, pH7.4, TFE as the co-solvent (0%, 2.5%, 5%, 7.5%, 10%, 12.5%, 15%). Difference CD spectra (D) as a function of TFE concentration (0%, 2.5%, 5%, 7.5%, 10%, 12.5%, 15%). The difference CD spectra are calculated subtracting the two individual peptide spectra from those of the mixture.

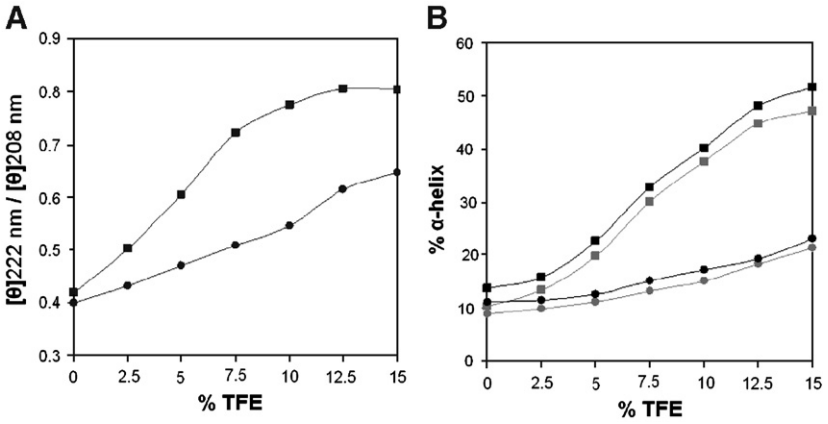

Fig. 2. (A) Ratio $[\theta]_{222\ nm}/[\theta]_{208\ nm}$ as a function of TFE concentration for HR1–25 (squared symbol), and for HR2–25 (filled circle). (B) Helical content from ellipticity value at 222 nm and 208 nm. Black square symbols: HR1–25 helical content at 222 nm; grey square symbols: HR1–25 helical content at 208 nm. Black filled circle: HR2–25 helical content at 222 nm; grey filled circle: HR2–25 helical content at 208 nm.

peptide residues. Blank, single peptide and mixture solutions were recorded in the same cell. Every spectrum is corrected for the blank.

TFE-titration and TFE-ACN studies were recorded at room temperature in a 1-mm cylindrical cell in the 194–260 nm range, at a 20-nm/min scan speed, spectral bandwidth 1 nm, response time 2 s, data pitch 0.2 nm. Melting curves and temperature were controlled by a Jasco Peltier system PTC-423 (Jasco, Japan). This system required strain-free rectangular cell (1 mm pathlength).

Higher resolution spectra were recorded in a 0.1-mm cylindrical cell, in the 180–260 nm range, at a 10-nm/min scan speed, spectral bandwidth 1 nm, response time 2 s, data pitch 0.1 nm, and resulted from the accumulation of two spectra.

Table 1
Structural estimate with MLR of spectra obtained during TFE titration

Sample	% TFE	Secondary structure estimate (%)					Analysis accuracy		
		α-helix	β-sheets	β-turns	Random coil	Sum	D	R	SE
HR1–25[a]	0	25.5		8.7	65.8	100.0	0.9983	0.9991	0.05
	2.5	30.2		7.5	62.2	99.9	0.9985	0.9992	0.03
	5	38.7		6.0	55.3	100.0	0.9989	0.9995	0.02
	7.5	52.3		3.0	44.6	99.9	0.9990	0.9995	0.02
	10	65.3			34.7	100.0	0.9582	0.9738	1.67
	12.5	65.0		0.8	34.2	100.0	0.9989	0.9995	0.04
	15	64.2	2.2	0.0	33.5	99.9	0.9989	0.9994	0.05
HR2–25[a]	0	21.0		12.2	66.8	100.0	0.9983	0.9992	0.04
	2.5	22.4		12.4	65.3	100.1	0.9981	0.9991	0.04
	5	24.0		12.0	64.1	100.1	0.9986	0.9993	0.03
	7.5	26.8		11.7	61.5	100.0	0.9985	0.9992	0.03
	10	29.9		10.8	59.3	100.0	0.9986	0.9993	0.02
	12.5	33.3		10.3	56.5	100.1	0.9989	0.9994	0.02
	15	36.8		9.5	53.7	100.0	0.9987	0.9993	0.02
1:1 Mixture[a]	0	23.4		10.3	66.4	100.1	0.9987	0.9993	0.13
	2.5	26.2		10.1	63.7	100.0	0.9988	0.9994	0.11
	5	32.5		8.9	58.6	100.0	0.9990	0.9995	0.08
	7.5	40.2		7.3	52.5	100.0	0.9992	0.9996	0.06
	10	47.4		5.6	47.0	100.0	0.9991	0.9995	0.07
	12.5	51.0		4.9	44.1	100.0	0.9989	0.9995	0.09
	15	54.4		3.8	41.8	100.0	0.9990	0.9995	0.10
Difference spectra[a]	0	22.9		10.0	67.1	100.0	0.9913	0.9956	0.02
	2.5	24.7		11.7	63.6	100.0	0.9846	0.9923	0.03
	5	40.6		9.4	50.0	100.0	0.9814	0.9907	0.02
	7.5	41.7		9.8	48.5	100.0	0.9780	0.9889	0.02
	10	54.9		6.1	39.0	100.0	0.9863	0.9931	0.02
	12.5	49.3		6.5	44.2	100.0	0.9860	0.9930	0.02
	15	58.7		3.8	37.5	100.0	0.9948	0.9974	0.01

For HR1–25, using the whole set or the combination of α-helix, β-turn and random coil gave the same results in term of D, R, SE, so only the second analysis is reported. MLR did a real poor job with HR1–25 10% TFE spectrum; best estimate with two of the reference spectra (α-helix and random coil) has, however, a high SE.

[a] For HR2–25, 1:1 mixture and difference spectra, good results were obtained only with the combination of reference spectra for α-helix, β-turn and random coil.

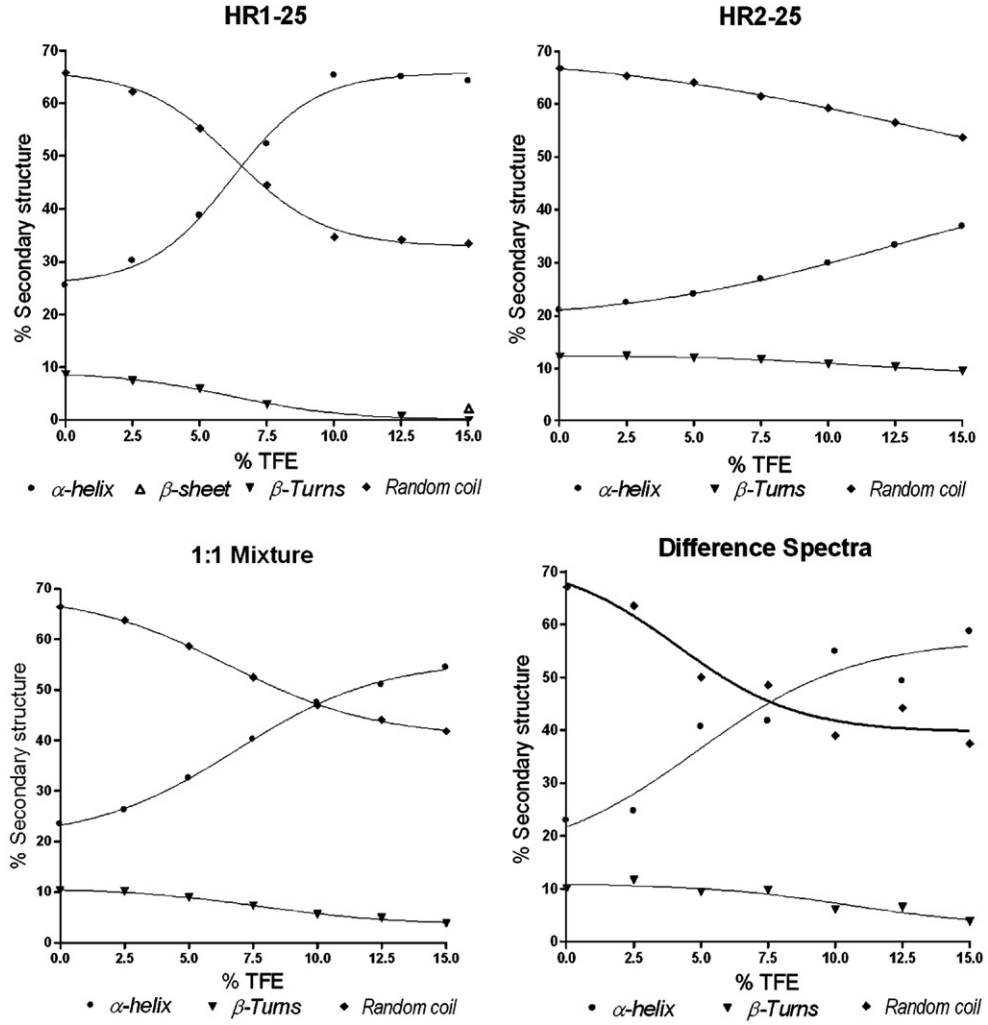

Fig. 3. Secondary structure content variations as a function of TFE concentration, as derived from multilinear regression analysis of CD spectra. A line shows a fit for data.

2.3. Preparation of sample solutions

Lyophilized peptides were synthesized by Primm (San Raffaele Biomedical Science Park, Milan, Italy) on the basis of the following sequences: HR1–25 TARLQLEARLQHLVAEILEREQSLA, HR2–25 SDVAAATNADLRTALA-RADHQKTLF. The peptide's purity, as supplied by Primm, was >95% for HR1–25 and >80% for HR2–25. Each peptide was dissolved in the appropriate buffer to yield a stock solution of 200 μM (titration studies) or 400 μM (high resolution spectra and melting curves).

Each stock solution was then diluted to the appropriate concentration (50 μM for most of the measurements, and 180 μM for the high resolution CD spectra) with buffer and, if necessary, the appropriate volume of solvent (TFE or ACN) to reach the expected solvent/buffer v/v percentage. All solutions were kept on ice throughout the experiment and each dilution was prepared just before analysis and then equilibrated to room (or otherwise stated) temperature.

2.4. Titration in TFE

50 μM peptides and 1:1 (molar ratio) mixture PBS solutions were titrated in the presence of 0%, 2.5%, 5%, 7.5%, 10%, 12.5%, and 15% TFE. The results are the average of three experiments for the single peptides, and of two experiments for the mixture and difference analysis. Difference spectra were obtained subtracting the addition of the two individual peptide curves from the spectrum of the mixture. Data of the individual peptide were converted to molar ellipticity to estimate the α-helix content at 222 nm and 208 nm (see Data Analysis); spectra in the range 240–200 nm in millidegrees were submitted to multilinear regression analysis.

2.5. TFE-ACN studies

50 μM peptides and 1:1 (molar ratio) mixture 10 mM phosphate buffer pH 5.5 were titrated in the presence of 10% and 15% of either TFE or ACN.

2.6. Temperature and salts

Four different buffers were used to dilute a stock solution of 200 μM in PBS of each peptide: PBS, 10 mM phosphate buffer pH 7.4; 10 mM phosphate buffer

Table 2
Increments in the α-helical content during titration[a]

Sample	Method of estimate		
	MLR	$[\theta]_{222\ nm}$	$[\theta]_{208\ nm}$
HR1–25	39	37	38
HR2–25	16	12	12
Mixture	31	n.a.	n.a
Difference spectra	36	n.a.	n.a.

[a] Variations expressed as the difference in α-helix content measured at 15% TFE and 0%TFE.

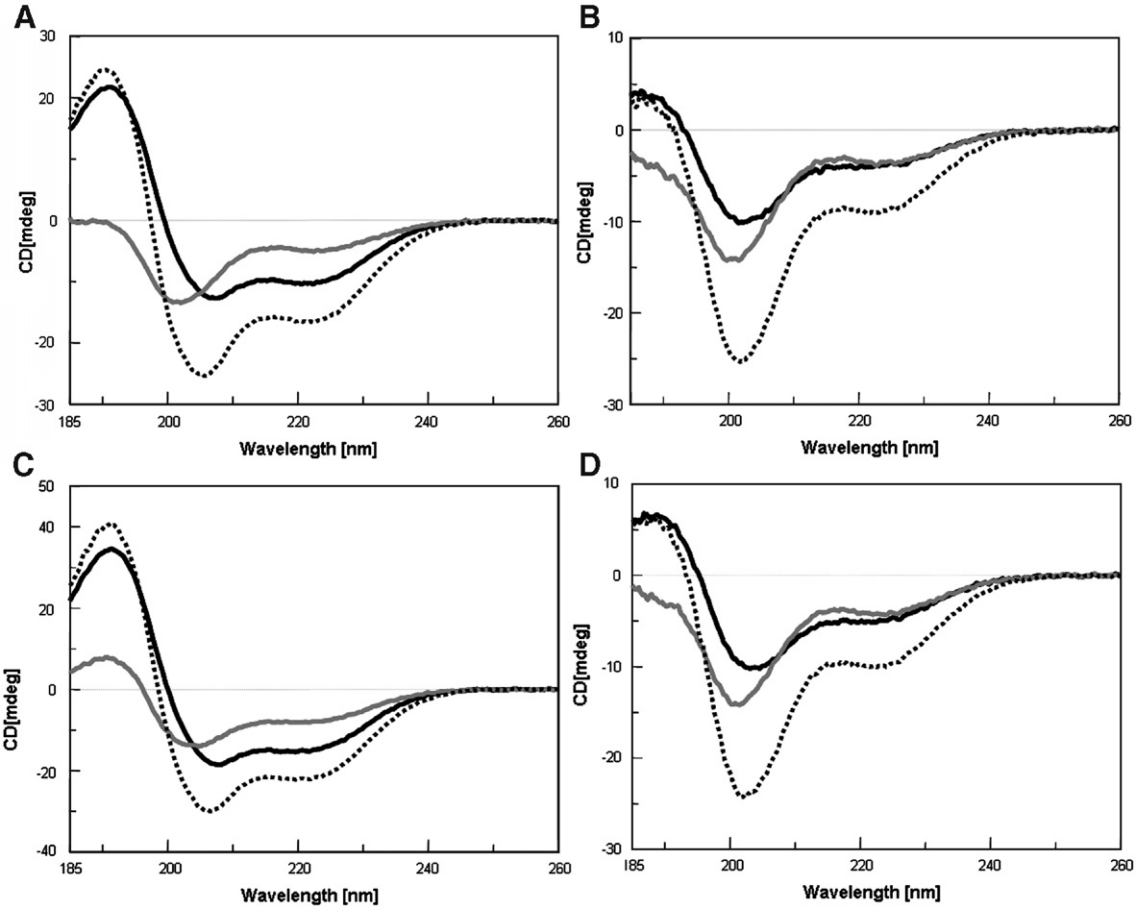

Fig. 4. (A) HR1–25 (black line), HR2–25 (grey line) and 1:1 mixture (dotted line) in 10 mM phosphate buffer pH 5.5 10% TFE. (B) HR1–25 (black line), HR2–25 (grey line) and 1:1 mixture (dotted line) in 10 mM phosphate buffer pH 5.5 10% ACN. (C) HR1–25 (black line), HR2–25 (grey line) and 1:1 mixture (dotted line) in 10 mM phosphate buffer pH 5.5 15% TFE. (D) HR1–25 (black line), HR2–25 (grey line) and 1:1 mixture (dotted line) in 10 mM phosphate buffer pH 5.5 15% ACN.

Na_2SO_4 68.5 mM, KCl 2.7 mM pH 7.4; 10 mM phosphate buffer Na_2SO_4 68.5 mM, KCl 2.7 mM 10% TFE pH 7.4. Spectra of 50 μM solutions of each peptide and the mixture were recorded at 4 °C every 10 min for 60 (phosphate buffer) to 90 min (other conditions). Spectra were accumulated.

2.7. Melting curves

Temperature denaturation midpoints (melting temperature, T_m) for the peptides and the 1:1 mixture in 100% PBS or PBS with 10% TFE were determined by following the change in ellipticity at 222 nm from 4 to 90 °C in a 1-mm path length cell and a temperature increase rate of 2 °C/min. The results are the average of three experiments.

T_m in PBS and 10% TFE were determined on the maximum of the first derivative curves [5] obtained with the Jasco Spectra Analysis facilities.

Ellipticity readings for the single peptides were normalized to the fraction of peptide folded (f) using the standard equations: $f=([\theta]_{222}-[\theta]^{90})/([\theta]^{4}-[\theta]^{90})$, where $[\theta]^{4}$ and $[\theta]^{90}$ represent the ellipticity values for the fully folded (at 4 °C) and fully unfolded (at 90 °C) species, respectively. $[\theta]_{222}$ is the observed ellipticity at 222 nm at any temperature. T_m was determined as the temperature at which the peptide is 50% unfolded [7].

2.8. Data analysis

The $[\theta]_{222\ nm}/[\theta]_{208\ nm}$ ratio is a rough but useful parameter to deduce coiled-coil and α-helical propensity; a value between 0.8 and 0.95 is symptomatic of an α-helix, and becomes higher in the presence of a coiled-coil conformation (interacting α-helices) [8].

α-helical content was estimated using the equation for the chain length dependence of an α-helix, assuming a molar ellipticity value of $[\theta]_{222\ nm\text{-}100\%}=-40000\times(1-4.6/N)=32333$ deg cm^2 dmol^{-1} for a 100% α-helical peptide [9] where N is the number of peptide bonds [10] (N=24 for each peptide). This value was compared to α-helix content evaluated from the ellipticity at 208 nm: $\%\alpha\text{-helix}_{208\ nm}=100\ ([\theta]_{208\ nm}-(-4000)/(-33000-(-4000))$. This estimate [11] assumes that the contribution of β-sheets and random coil to the signal at 208 nm is −4000 deg cm^2 dmol^{-1}, while the contribution of α-helix is assumed to be −33000 deg cm^2 dmol^{-1}.

Secondary structure was analysed performed using freeware software packages available on the web, namely CDPro [12] (http://lamar.colostate.edu/~sreeram/CDPro/main.html) and Multi Linear Regression (MLR), available at http://www2.umdnj.edu/cdrwjweb [13,14]. CD data submitted to the analysis were collected with absorbance below 1. The output files were converted into

Table 3
Ratio $[\theta]_{222\ nm}/[\theta]_{208\ nm}$ as a function of solvent concentration

Sample	10% organic solvent		15% organic solvent	
	10% TFE	10% ACN	15% TFE	15% ACN
HR1–25	0.81	0.54	0.82	0.60
HR2–25	0.57	0.46	0.67	0.52
Mixture[a]	0.71	0.52	0.75	0.56

[a] As a ratio is involved, and the values of concentration, residues and pathlength annul each other, ratios have been calculated from millidegrees value of the mixture spectra.

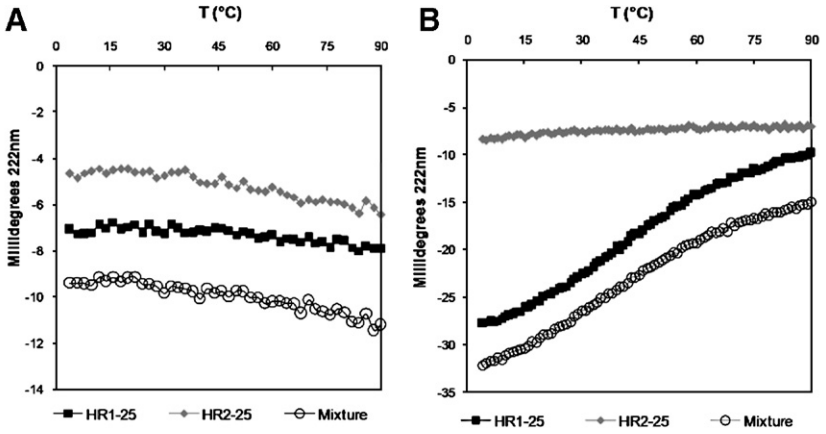

Fig. 5. Thermal denaturation in PBS 0% TFE (A) and in PBS 10% TFE (B). Unfolding curves of the individual peptides and 1:1 mixture of the two peptides.

MS Excel data sheets or into GraphPad Prism 4.0 files to manage statistics and graphics on data.

CDPro was chosen because it allows deconvolution of CD data with three different programs (CONTIN/LL, SELCON3 and CDSSTR) that run on multiple basis sets. Basis sets used in the analysis are 1, 3, 4, 6, 7 (see ref. [12] for full description) because results should be comparable as the secondary structure fractions assignments from crystallography data are identical. Each spectrum, expressed in molar ellipticity, was analysed with the three algorithms and with the five different basis sets. Results were averaged among basis sets and among programs. Structures estimated included α-helix, regular (R) and distorted (D), β-sheet, regular (R) and distorted (D), β-turn and non-ordered structure.

For the analysis with MLR the reference spectra from Brahms and Brahms [15] (as supplied by the web site cited) for α-helix, β-sheet, β-turn and random coil were used. These spectra are: the α-helix (sperm whale myoglobin corrected for the contributions of turns and random coil and normalized to 1.0) in 0.1 M NaF, pH 7; β-sheet (poly(lys-leu)n, in 0.5 M NaF at pH 7); β-turn (poly(ala_2, $gly)_n$ in water multiplied by 0.5); and random coil (poly(pro-lys-leu-lys-leu)$_n$ in salt free solution). The maximum range permitted by this data set is 240–178 nm (240–200 nm in this case). CD spectra in millidegrees (not corrected for concentration) were analysed. Best fit among different combinations of reference spectra was evaluated with the following criteria: (1) no negative fractions, (2) sums of fraction close to 100%, (3) the highest coefficient of determination (*D*), the highest coefficient of multiple correlation (*R*) and the lowest standard error of estimate (SE).

3. Results and discussion

3.1. Titration in TFE

The aim of the titration study was to investigate the peptides' propensity to adopt an α-helix conformation already suggested by bioinformatics studies [4]. Titration in TFE was carried out in PBS at 0%, 2.5%, 5%, 7.5%, 10%, 12.5% and 15% TFE. The maximum percentage of TFE is 15%, as too high a concentration of this solvent may favour intramolecular order, but it may also be unfavourable to intermolecular aggregation and thwart the investigation of complex formation. Moreover, with some peptides a plateau value in α-helical content is reached at TFE concentration higher than 12%, but such plateaus do not represent full conversion into α-helix [16].

A significant conformational change was observed in HR1–25 (Fig. 1, panel A) on increasing the concentration of TFE. The shape of the spectra, clearly that of a disordered structure in aqueous buffer, changed and presented two negative bands at 208 nm and 222 nm, characteristic of an α-helix structure, at the

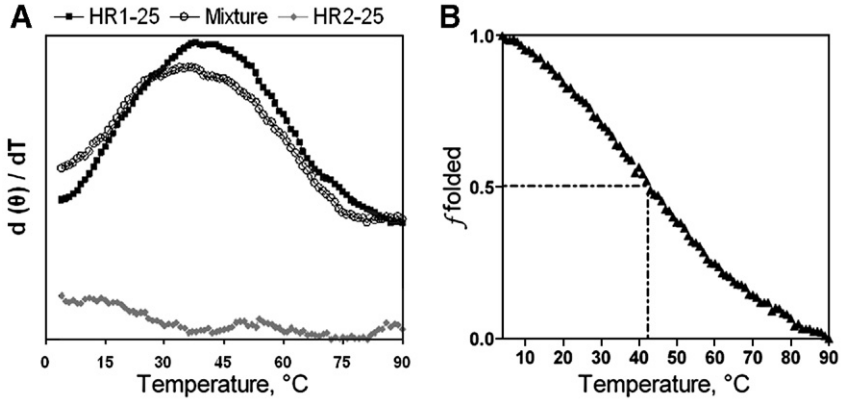

Fig. 6. Melting temperature in PBS 10% TFE. (A) First order derivatives [6] of the unfolding curves of the two individual peptides and the 1:1 mixture; the maximum of the derivative allow the determination of T_m: 42 °C for HR1–25, and 37 °C for the mixture. HR2–25 is not affected by thermal denaturation. (B) Unfolding curves of HR1–25 expressed as fraction folded *f*. T_m was determined as the temperature at which 50% of the peptide is unfolded [7]. T_m is calculated as the temperature at which 50% of the peptide is still folded: 42 °C.

highest TFE concentration used. On the contrary, HR2–25 (Fig. 1, panel B) underwent minor conformational changes during titration and even at 15% TFE the spectrum revealed a mostly disordered structure. The behaviour of the 1:1 mixture (Fig. 1, panel C) upon increasing TFE concentration appears close to that of HR1–25 peptides as shown by the clean appearance of the negative bands at 208 nm and 222 nm. The negative band at 222 nm, however, was less intense than expected, as if the mixture suffered from the presence of the more disordered peptide, HR2–25. Interestingly, superimposition of the spectra recorded at increasing TFE concentration shows a clean conserved isosbestic point at 203 nm for each peptide and for the mixture, revealing a two-state transition from a random coil (disordered) conformation to a high α-helical content.

In terms of detecting an interaction between the two peptides, difference spectra were monitored during titration (Fig. 1, panel D). A difference spectrum is obtained as the difference between the mixture signal and the sum of the contribution of the two individual peptides. In this case, a not negligible signal was observed at every TFE percentage, but even at 15% TFE the contribution at 208 nm is only about 12% the signal of the mixture: less than usually detected in similar models [5,7].

To quantify the extent of these conformational changes, different analyses were undertaken.

Firstly, the $[\theta]_{222\ nm}/[\theta]_{208\ nm}$ ratio was evaluated (Fig. 2, panel A) for HR1–25 and HR2–25: while it increases twofold for HR1–25 at the highest concentration of TFE (0.8), the increase is less marked for HR2–25 (0.6 at 15% TFE). The $[\theta]_{222\ nm}/[\theta]_{208\ nm}$ ratio is normally interpreted as an indicator of coiled-coil formation. It is assumed that a ratio between 0.8 and 0.95 (close to 1) is representative of single chain α-helix, while a ratio above 1 is symptomatic of the coiled-coil formation in peptides prone to adopt those conformations [8]. In the conditions used, the ratio revealed an increase in the α-helical content of the individual peptide, but not the association of chains in solutions as the ratio did not exceed the value (1) expected for a coiled coil structure.

Then, the α-helix fraction (as a percentage) was estimated at 222 nm and 208 nm as described in Materials and methods (Fig. 2, panel B). The two values were in agreement and showed a common response to TFE for each peptide. Thus, about half the amino acid residues should be involved in the α-helix structure for the HR1–25 peptide, while fewer residues of the HR2–25 peptide are in α-helix conformation.

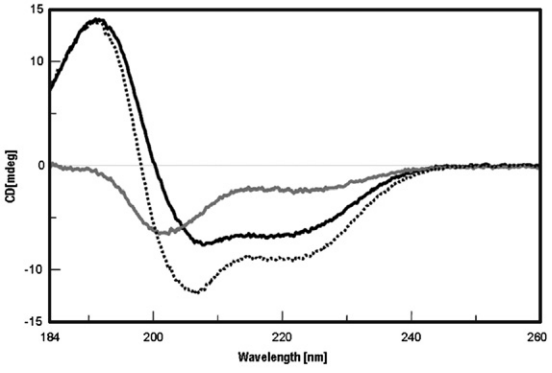

Fig. 7. HR1–25 180 μM (black line), HR2–25 180 μM (grey line) and 1:1 mixture (dotted line) in 10 mM phosphate buffer pH 7.4 10% TFE. Spectra were recorded in a 0.01-cm pathlength cell, scan speed 10 nm/min, bandwidth 1.

Table 4
Summary of secondary structure fraction obtained with CDPro analysis

Program	Helix[a]	Sheets[a]	Turns	Non Ordered	Sum
HR1–25					
CDSSTR	0.516	0.098	0.136	0.247	0.997
CONTIN/LL	0.469	0.101	0.162	0.267	1.000
SELCON3	0.469	0.109	0.165	0.261	1.005
Average	0.485	0.103	0.155	0.258	1.001
St. dev.	0.022	0.005	0.013	0.009	0.004
HR2–25					
CDSSTR	0.201	0.192	0.241	0.365	0.998
CONTIN/LL	0.202	0.111	0.176	0.510	1.000
SELCON3	0.179	0.172	0.199	0.434	0.984
Average	0.194	0.158	0.205	0.436	0.994
St. dev.	0.011	0.035	0.027	0.060	0.007

[a] Helix and Sheets fractions are the average between regular and distorted α-helix and between regular and distorted β-sheet.

Finally, a secondary structure analysis was performed. As the exact protein concentration cannot be established in the case of the 1:1 mixture solutions and the difference spectra, because the exact number of residues involved is unknown, MLR method was chosen, even though the limits of an unconstrained fit based on linear regression has been widely reviewed (see, for example, ref. [13,14,17]). The results of the analysis of the individual peptides, the mixture and the difference spectra are summarised in Table 1. The secondary structure changes as a function of TFE percentage for each sample are shown in Fig. 3. MLR seems to overestimate the absolute structure content by about 10% with respect to the previous analyses. As far as conformational changes are concerned, the crucial parameters were the maximum conformational changes occurring between 0% and 15% TFE (Table 2). For HR1–25 and HR2–25, the difference in the α-helix content determined by MLR was compared to that evaluated by ellipticity value at 222 and 208 nm. Even if MLR still seemed to slightly overestimate α-helix content in HR2–25, the quantified conformational changes were in good agreement. This gives reliability to the estimate of the entity of conformational variation undergone by the mixture that is translated into a conformational change of the non-covalent complex of HR1–25 and HR2–25 as revealed by the analysis on the difference spectra, even if this conformational change is small. Our group already noted the formation of this complex [6], as confirmed by an NPAGE study [6]. Mixing HR1–25 with increasing amounts of HR2–25, up to 1/1 molar ratio showed the formation of a simple hetero dimer, eventhough the possible presence of multimers was monitored. The higher order oligomers should arise from the binding of the irregular parts of the peptides, in addition to the helix–helix dimer formation. Recently, another work [21] on longer peptides derived from the same gH regions achieved similar results, but many more CD data were collected in the present investigation by working further in the UV range.

TFE is widely used in conformational studies because it promotes intramolecular hydrogen bonds in spite of intermolecular interaction with water molecules thereby enhancing α-helix formation [17–19]. Moreover, as TFE lowers the polarity of the solution, the environmental changes explored by the peptides resemble those of the native sequences during the fusion process. Indeed, similar studies on HR sequences and fusion peptides mimicking sequences used TFE in circular dichroism analysis [6,7,20,21]. So, the effect of 10% and 15% TFE was compared to that of 10% and 15% ACN, the latter solvent being less efficient in stabilizing ordered structures (Fig. 4). Shapes of the spectra revealed a stabilization of the random conformation to the detriment of α-helix content. This is particularly true for HR1–25, that has a high content of α-helix in the presence of 10% and 15% TFE. The $[\theta]_{222\ nm}/[\theta]_{208\ nm}$ ratio confirmed the transitions described for HR1–25, HR2–25 and the 1:1 mixture, as reported in Table 3. These spectra were obtained from peptides at pH=5.5 either in ACN or TFE. The fact that pH did not affect the structural content of the two peptides is consistent with the finding that the fusion process in which gH participates does not strictly depend on a decrease of pH [22].

3.2. Denaturation curves

The ellipticity values of HR1–25, HR2–25 and the 1:1 mixture at 222 nm were monitored in 100% PBS and PBS with 10% TFE. Thermal denaturation experiments in 100% PBS solution did not significantly affect the θ_{222} CD values because the peptides, singly and in the 1:1 mixture, assumed an almost disordered structure in those experimental conditions. A slight decrease in ellipticity was observed but it was associated with "fraying" of the ends of the peptides in solutions (Fig. 5, panel A). In the presence of 10%TFE, HR2–25 CD signal was still not affected by thermal denaturation, whereas HR1–25 and the mixture revealed a significant decrease of the ellipticity absolute value at 222 nm (Fig. 5, panel B). The first derivatives curve of HR1–25 showed a maximum at 42 °C, the T_m of the peptide in this condition, while the 1:1 mixture showed a T_m of 37 °C (Fig. 6, panel A). This is quite surprising, because stabilization to thermal denaturation is expected as a consequence of formation of a complex between the two peptides. However the T_m of the mixture is relatively close to that of HR1. Thus the behaviour of the mixture does not resemble the mean behaviour of the two peptides in the same solution, even though triggered by the

Table 5
Structural estimate of HR1–25 180 μM phosphate buffer 10 mM, 10% TFE[a]

Basis set[b]	Helix (R)	Helix (D)	Sheets (R)	Sheets (D)	Turns	Non-ordered	Sum	RMSD[c]	NRMSD[d]
CDSSTR									
Basis 1	0.313	0.194	0.044	0.047	0.168	0.230	0.996	0.163	0.037
Basis 3	0.340	0.191	0.047	0.047	0.132	0.239	0.996	0.192	0.037
Basis 4	0.325	0.178	0.062	0.048	0.131	0.250	0.994	0.204	0.042
Basis 6	0.340	0.190	0.045	0.045	0.135	0.244	0.999	0.166	0.032
Basis 7	0.331	0.178	0.060	0.044	0.115	0.270	0.998	0.166	0.034
mean	0.330	0.186	0.052	0.046	0.136	0.247	0.997		
St. dev.	0.011	0.008	0.009	0.002	0.019	0.015	0.002		
Average	0.516		0.098		0.136	0.247	0.997		
CONTIN/LL									
Basis 1	0.284	0.178	0.054	0.054	0.166	0.264	0.999	0.132	0.030
Basis 3	0.301	0.178	0.042	0.055	0.161	0.264	1.000	0.116	0.022
Basis 4	0.289	0.173	0.050	0.057	0.162	0.269	1.000	0.085	0.018
Basis 6	0.302	0.177	0.040	0.055	0.162	0.264	1.000	0.112	0.022
Basis 7	0.293	0.171	0.047	0.053	0.160	0.276	1.000	0.084	0.017
mean	0.294	0.175	0.047	0.055	0.162	0.267	1.000		
St. dev.	0.026	0.025	0.044	0.026	0.075	0.005	0.000		
Average	0.469		0.101		0.162	0.267	1.000		
SELCON3									
Basis 1	0.291	0.176	0.060	0.056	0.178	0.259	1.020	0.872	*0.197*
Basis 3	0.305	0.176	0.059	0.051	0.161	0.254	1.006	0.934	*0.181*
Basis 4	0.291	0.169	0.049	0.056	0.162	0.268	0.995	0.967	*0.200*
Basis 6	0.304	0.175	0.061	0.052	0.162	0.253	1.007	0.967	*0.188*
Basis 7	0.292	0.167	0.050	0.053	0.163	0.273	0.998	0.966	*0.200*
mean	0.297	0.173	0.056	0.054	0.165	0.261	1.005		
St. dev.	0.007	0.004	0.006	0.002	0.007	0.009	0.010		
Average	0.469		0.109		0.165	0.261	1.005		

So far, Selcon3 for HR1–25 gave poor results. However, this parameter is only a symptom of similarity between the two mentioned spectra, and a good NMRSD does not necessary imply a better estimate of fraction. So the final estimate reported in Table 4 include all the values.

[a] Structures estimated are α-helix, regular (R) and distorted (D), β-sheet, regular (R) and distorted (D), β-turn and non-ordered structure.

[b] For details about basis spectra, see ref. [12].

[c] Root Mean Square Difference.

[d] Normalized Root Mean Square Difference is a measure of the goodness of fit between calculated and experimental spectra.

strong propensity of HR1–25 to adopt an α-helical conformation. Denaturation curves were also expressed in terms of fraction folded (f) (Fig. 6, panel B). T_m was calculated as the temperature at which the peptide is 50% folded. The values obtained for HR1–25 were consistent with those calculated on the derivative curves.

3.3. Fully folded peptides: different buffers at 4 °C

A low temperature is assumed to stabilize the folding of the peptides in their most favourable conformation in a particular environment. To this purpose, four different buffers were tested and the spectra followed every 10 min for 60 to 90 min so as not to underestimate the need for time-dependent folding at low temperature. The peptides and the mixture spectra collected throughout the experiment were identical, so spectra were accumulated (data not shown) to obtain low noise content spectra suitable for structure estimation. However, the Peltier system has a strong intrinsic UV absorbance, so the spectra are meaningful only down to 220 nm, after which the information content is too low to yield meaningful estimates. The comparison of the spectra recorded did not disclose any particular conformational variation upon buffer differences, and buffer containing Na_2SO_4 instead of NaCl maintained the propensity to TFE-induced conformational changes.

3.4. Concentration

In order to record higher resolution spectra, the concentration was raised to 180 μM for both peptides and the 1:1 (molar ratio) mixture. To collect high information content spectra, phosphate buffer with 10% TFE and 0.01 cm pathlength cell were used. TFE was introduced to increase the α-helix fraction that is still the structure best estimated by deconvolution programs. Spectra (shown in Fig. 7) were analysed with CDPro in the 184–260 nm range, with the absorbance kept below 1. Averaged results among every basis set and every program are summarised in Table 4. The propensity of the two peptides was confirmed, as the estimates are consistent with data from titration studies.

The estimates of each program obtained with the five basis sets were comparable, and so were the average estimates of the three programs. The goodness of fit was reasonable even if the Normalised Root Mean Square Difference (NRMSD, see Tables 5 and 6) between the observed and reconstructed spectra by the

Table 6
Structural estimate of HR2–25 180 μM phosphate buffer 10 mM, 10% TFE[a]

Basis set[b]	Helix (R)	Helix (D)	Sheets (R)	Sheets (D)	Turns	Non Ordered	Sum	RMSD[c]	NRMSD[d]
CDSSTR									
Basis 1	0.053	0.138	0.114	0.085	0.299	0.307	0.996	0.225	*0.120*
Basis 3	0.089	0.149	0.112	0.095	0.272	0.285	1.002	0.391	*0.178*
Basis 4	0.080	0.126	0.124	0.093	0.260	0.313	0.996	0.344	*0.149*
Basis 6	0.076	0.113	0.107	0.074	0.201	0.430	1.001	0.316	*0.144*
Basis 7	0.074	0.107	0.092	0.063	0.171	0.488	0.995	0.283	*0.123*
mean	0.074	0.127	0.110	0.082	0.241	0.365	0.998		
St. dev.	0.013	0.017	0.012	0.013	0.053	0.089	0.003		
Average	0.201		0.192		0.241	0.365	0.998		
CONTIN/LL									
Basis 1	0.096	0.110	0.043	0.067	0.227	0.456	0.999	0.127	0.068
Basis 3	0.134	0.141	0.036	0.082	0.235	0.372	1.000	0.132	0.060
Basis 4	0.069	0.126	0.125	0.089	0.232	0.359	1.000	0.129	0.056
Basis 6	0.093	0.079	0.019	0.042	0.096	0.671	1.000	0.128	0.058
Basis 7	0.073	0.091	0.022	0.028	0.092	0.694	1.000	0.096	0.042
mean	0.093	0.109	0.049	0.062	0.176	0.510	1.000		
St. dev.	0.026	0.025	0.044	0.026	0.075	0.162	0.000		
Average	0.202		0.111		0.176	0.510	1.000		
SELCON3									
Basis 1	0.076	0.099	0.076	0.067	0.240	0.433	0.991	1.018	*0.543*
Basis 3	0.099	0.119	0.081	0.087	0.247	0.368	1.001	1.515	*0.689*
Basis 4	0.081	0.106	0.141	0.088	0.191	0.354	0.961	0.530	*0.230*
Basis 6	0.093	0.074	−0.003	0.037	0.105	0.712	1.018	0.501	*0.228*
Basis 7	0.063	0.073	0.091	0.055	0.118	0.582	0.982	0.234	*0.102*
mean	0.080	0.099	0.097	0.074	0.199	0.434	0.984		
St. dev.	0.014	0.020	0.052	0.022	0.066	0.154	0.021		
Average	0.179		0.172		0.199	0.434	0.984		

So far, CDSSTR and Selcon3 for HR2–25 gave poor results. However, this parameter is only a symptom of similarity between the two mentioned spectra, and a good NMRSD does not necessary imply a better estimate of fraction. So the final estimate reported in Table 4 include all the values.

[a] Structures estimated are α-helix, regular (R) and distorted (D), β-sheet, regular (R) and distorted (D), β-turn and non-ordered structure.

[b] For details about basis spectra, see ref. [12].

[c] Root Mean Square Difference.

[d] Normalized Root Mean Square Difference is a measure of the goodness of fit between calculated and experimental spectra.

fitting algorithm was quite high. However, a good agreement between the observed and the calculated spectrum does not unambiguously mean that the structural estimate is accurate, especially if small peptides, as in this case, are analysed with protein databases as references.

4. Conclusions

Revealing the secondary structure adopted by a model peptide in solution is a means to grasp the mechanism of folding, so intriguingly investigated because of the deep relationship between folding, environmental condition and, possibly, function. Attempts to predict secondary structure from amino acid sequence could be useful, but most algorithms do not include solvent effect. Circular dichroism studies are a straightforward way to highlight the secondary structure of peptides and proteins in solution and their variations. In the case of HR1–25 and HR2–25 peptides, propensity to assume an α-helix conformation was confirmed by titration study in TFE; comparison of ACN and TFE spectra, however, revealed as strong dependence of conformation on local environment. The effect of environment on secondary structure has been widely studied showing a strong reliance on neighbouring amino acids and local environment (solvent and solutes) [17–19], a dependence not really included in common bioinformatic prediction.

This study disclosed a strong propensity to adopt a α-helix, in particular for HR1–25, as solvent polarity decreases in a two-state transition model. This tendency was assessed by the broadly different information that can be extrapolated from CD spectra. This study processed data using parameters like the ellipticity value at 222 nm or the $[\theta]_{222\ nm}/[\theta]_{208\ nm}$ ratio that are as widely used as critically accepted. Only the complete spectrum contains all the structural information on the peptide (or protein) analysed. Those parameters, however, if conveniently supported, help to reveal the propensity to conformational variation as a function of different environmental conditions that is a real concern when investigating a chemical reconstructed model of a more complex biological system. The structural estimate obtained by CDPro and MLR should be interpreted in this light. Making every effort to work in the best spectroscopic and "deconvolution" conditions, this is actually quite difficult if a native environment has to be maintained or reproduced. So far, a program, like MLR, though not as sophisticated as the newly available algorithms, has been chosen for its advantages in estimating secondary structure from spectra with unknown concentration, such as the difference and mixture spectra, and because of a reference set which is very small, but contains peptide spectra. On the other hand, CDPro offers three refined programs with multiple basis sets that may also include denaturated and membrane proteins, but require high resolution spectra (at least close to 180 nm) and a well-known concentration of sample to give a reliable estimate of structure. However, the structural features of a peptide may be not well represented by protein reference sets, and vice versa, and the analysis could be biased. Despite the questionable limits and assumptions of the methods used, CDPro and MLR, like all the other parameters evaluated, quantitatively express what is qualitatively illustrated in the CD spectra: the structure of the two peptides is solvent-dependent, and appropriate environment conditions promote α-helix conformations that may be differently involved in the different steps of either the fusion process involving the native protein, or the inhibition of the fusion mechanism involving the synthetic peptides.

Acknowledgments

This work was supported by a grant from MIUR, Rome, Italy.

References

[1] P.M. Colman, M.C. Lawrence, The structural biology of type I viral membrane fusion, Nat. Rev., Mol. Cell Biol. 4 (2003) 309–319.
[2] R.M. Epand, Fusion peptides and the mechanism of viral fusion, Biochim. Biophys. Acta 1614 (2003) 116–121.
[3] T. Gianni, P.L. Martelli, R. Casadio, G. Campadelli-Fiume, The ectodomain of herpes simplex virus glycoprotein H contains a membrane alpha-helix with attributes of an internal fusion peptide, positionally conserved in the herpesviridae family, J. Virol. 79 (2005) 2931–2940.
[4] T. Gianni, L. Menotti, G. Campadelli-Fiume, A heptad repeat in herpes simplex virus 1 gH, located downstream of the alpha-helix with attributes of a fusion peptide, is critical for virus entry and fusion, J. Virol. 79 (2005) 7042–7049.
[5] S. Liu, G. Xiao, Y. Chen, Y. He, J. Niu, C.R. Escalante, H. Xiong, J. Farmar, A.K. Debnath, P. Tien, S. Jiang, Interaction between heptad repeat 1 and 2 regions in spike protein of SARS-associated coronavirus: implications for virus fusogenic mechanism and identification of fusion inhibitors, Lancet 363 (2004) 938–947.
[6] T. Gianni, A. Piccoli, C. Bertucci, G. Campadelli-Fiume, Heptad repeat 2 in herpes simplex virus 1 gH interacts with heptad repeat 1 and is critical for virus entry and fusion, J. Virol. 80 (2006) 2216–2224.
[7] B. Tripet, M.W. Howard, M. Jobling, R.K. Holmes, KV. Holmes, R.S. Hodges, Structural characterization of the SARS-coronavirus spike S fusion protein core, J. Biol. Chem. 279 (2004) 20836–20849.
[8] R.S. Kiss, C.M. Kay, R.O. Ryan, Amphipathic alpha-helix bundle organization of lipid-free chicken apolipoprotein A-I, Biochemistry 38 (1999) 4327–4334.
[9] N.J. Greenfield, S.E. Hitchcock-De Gregori, Conformational intermediates in the folding of a coiled-coil model peptide of the N-terminus of tropomyosin and alpha alpha-tropomyosin, Protein Sci. 2 (1993) 1263–1273.
[10] W. Shalongo, E. Stellwagen, Dichroic statistical model for prediction and analysis of peptide helicity, Proteins 28 (1997) 467–480.
[11] N.J. Greenfield, G.D. Fasman, Computed circular dichroism spectra for the evaluation of protein conformation, Biochemistry 8 (1969) 4108–4116.
[12] N. Sreerama, R.W. Woody, Estimation of protein secondary structure from circular dichroism spectra: comparison of CONTIN, SELCON, and CDSSTR methods with an expanded reference set, Anal. Biochem. 287 (2000) 252–260.
[13] N.J. Greenfield, Analysis of circular dichroism data, Methods Enzymol. 383 (2004) 282–317.
[14] N.J. Greenfield, Methods to estimate the conformation of proteins and polypeptides from circular dichroism data, Anal. Biochem. 235 (1996) 1–10.
[15] S. Brahms, J. Brahms, Determination of protein secondary structure in solution by vacuum ultraviolet circular dichroism, J. Mol. Biol. 138 (1980) 149–178.
[16] K.R. Shoemaker, R. Fairman, D.A. Schultz, A.D. Robertson, E.J. York, J.M. Stewart, R.L. Baldwin, Side-chain interactions in the C-peptide helix: Phe 8-His 12+, Biopolymers 29 (1990) 1–11.
[17] W.C. Johnson Jr., Protein secondary structure and circular dichroism: a practical guide, Proteins 7 (1990) 205–214.

[18] L. Zhong, W.C. Johnson Jr., Environment affects amino acid preference for secondary structure, Proc. Natl. Acad. Sci. U. S. A. 89 (1992) 4462–4465.
[19] D.V. Waterhous, W.C. Johnson Jr., Importance of environment in determining secondary structure in proteins, Biochemistry 33 (1994) 2121–2128.
[20] S. Galdiero, A. Falanga, M. Vitiello, H. Browne, C. Pedone, M. Galdiero, Fusogenic domains in herpes simplex virus type 1 glycoprotein H, J. Biol. Chem. 280 (2005) 28632–28643.
[21] S. Galdiero, M. Vitiello, M. D'Isanto, A. Falanga, C. Collins, K. Raieta, C. Pedone, H. Browne, M. Galdiero, Analysis of synthetic peptides from heptad-repeat domains of herpes simplex virus type 1 glycoproteins H and B, J. Gen. Virol. 87 (2006) 1085–1097.
[22] T. Gianni, G. Campadelli-Fiume, L. Menotti, Entry of herpes simplex virus mediated by chimeric forms of nectin1 retargeted to endosomes or to lipid rafts occurs through acidic endosomes, J. Virol. 78 (2004) 12268–12276.